Correlated Two-Electron Momentum Spectra for Strong-Field Nonsequential Double Ionization of He at 800 nm

A. Rudenko,[1] V. L. B. de Jesus,[2] Th. Ergler,[1] K. Zrost,[1] B. Feuerstein,[1] C. D. Schröter,[1] R. Moshammer,[1] and J. Ullrich[1]

[1]*Max-Planck-Institut für Kernphysik, Saupfercheckweg 1, D-69117 Heidelberg, Germany*
[2]*Centro Federal de Educação Tecnológica de Química de Nilópolis/RJ,*
Rua Lucio Tavares 1045, Centro-Nilópolis-26530-060, Rio de Janeiro, Brazil

We report on a kinematically complete experiment on nonsequential double ionization of He by 25 fs 800 nm laser pulses at 1.5 PW/cm^2. The suppression of the recollision-induced excitation at this high intensity allows us to address in a clean way direct $(e, 2e)$ ionization by the recolliding electron. In contrast with earlier experimental results, but in agreement with various theoretical predictions, the two-electron momentum distributions along the laser polarization axis exhibit a pronounced V-shaped structure, which can be explained by the role of Coulomb repulsion and typical $(e, 2e)$ kinematics.

Nonsequential double ionization (NSDI) of atoms by intense linearly polarized laser fields has remained in the focus of strong-field physics as one of the central and most controversial topics despite intensive experimental and theoretical research for more than two decades (see [1] for a recent review). Its attractiveness mainly originates from the fact that this phenomenon represents a uniquely clean example of electron-electron correlation enforced by the external field, while at the same time enhancing the coupling efficiency between the laser light and two electrons by many orders of magnitude. Though most of the experimental findings are in good overall agreement with a semiclassical "recollision" model [2,3], where the first electron is set free close to the maximum of the oscillating laser field, is driven back to its parent ion when the field changes its sign, and either ionizes or excites the second electron, the current theoretical understanding of NSDI is far from being complete. While the most advanced semianalytical quantum-mechanical approaches based on the so-called "strong-field approximation," known also as "S-matrix theory" [4] achieve reasonable agreement with the measured double-ionization yields [5] and account for the major features of the existing differential data (e.g., a characteristic double-hump structure in the recoil-ion momentum distribution) [6,7], they experience severe difficulties trying to account for the realistic atomic structure (role of the Coulomb potential, structure of the bound excited states, etc.), which was experimentally found to play an important role [8,9]. Recent classical models (see [10] and references therein), though providing an intuitive insight into the two-electron dynamics within the recollision scenario, suffer from a similar problem, and, in addition, fail to predict the ionization rates due to their neglect of the quantum nature of the first ionization step.

The most accurate and reliable theoretical description of NSDI can be achieved by numerically solving the time-dependent Schrödinger equation (TDSE). However, fully dimensional calculations for two active electrons at optical or near-infrared wavelengths, where most of the experiments have been performed, are still computationally challenging [11], and single-active electron models, which can reliably predict fully differential rates for single ionization (see, e.g., [12]), fail severely for the case of NSDI. As a consequence, numerical solutions of the TDSE are often performed within reduced dimensionality (see [13] for one-, [14] for two-, and [15] for "one-plus-one"-dimensional approximations). At shorter wavelengths one can solve the full-dimensional two-electron TDSE, since here the smaller spatial excursion of the freed electrons allows one to reduce the numerical grid size and, thus, computational demands [11,16].

All numerical calculations mentioned above were performed for the He atom. The explicit numerical solution of the two-electron TDSE for larger systems seems to be far beyond present capabilities. Therefore, NSDI of He represents the prototype two-electron strong-field-induced reaction and, thus, the only possible "meeting point" between theory and experiment. Unfortunately, helium being the "simplest" atom for the theoretical description is, at the same time, the most challenging one for experimental investigations. This is due to its huge two-electron ionization potential resulting in low double-ionization rates and setting severe vacuum requirements for coincidence studies. Therefore, compared to the heavier rare gases, where even fully differential data including correlated two-electron momentum distributions are currently available (see [17,18] for Ne and [19,20] for Ar) over a broad intensity range, the experimental situation for He is much more obscure. Until now intensity-dependent ion yields [21], recoil-ion momentum distributions [8,9,22], and total electron energy spectra [16,23] have been measured. The only set of fully differential data for strong-field He double ionization reported until now [9] has suffered from rather low statistical significance and a complicated background subtraction procedure.

In this Letter we present the results of a kinematically complete experiment on NSDI of He at an intensity of 1.5×10^{15} W/cm^2. Choosing this rather high intensity, we were able to observe this prototype reaction in a regime, where the most often discussed mechanism of NSDI, direct (*e, 2e*)-like ionization by the rescattering electron, becomes the dominant pathway. We observe a clear signature of Coulomb effects in the correlated two-electron longitudinal momentum pattern, settling a long-standing controversy in the theoretical models of NSDI, and provide benchmark data for theory.

Measurements were performed using a "reaction microscope" described in detail in [9]. We used linearly polarized 795 nm 25 fs (FWHM) laser pulses at 3 kHz repetition rate. The laser beam was focused to a spot size of ~5 μm onto the supersonic gas jet in the ultrahigh vacuum chamber (2×10^{-11} mbar). Created ions and electrons were guided to two position-sensitive channel plate detectors by weak electric (2 V/cm) and magnetic (7 G) fields applied along the laser polarization axis. From the time-of-flight and position on the detector the full momentum vectors of the recoil ions and electrons were calculated. The total ionization count rate was kept below 1/3 per laser shot, in order to avoid false coincidences. Superior momentum resolution along the laser polarization (longitudinal) axis was achieved reaching $\Delta P_\parallel < 0.02$ a.u. for both ions and electrons. Along the transverse directions (i.e., in the plane perpendicular to the laser polarization), the ion-momentum resolution varied from ~0.5 a.u. along the gas-jet direction to less than 0.1 a.u. in the direction perpendicular to the jet. The transverse momentum resolution for electrons was on a level of $\Delta P_\perp \sim 0.05$ a.u. (see [9] for details). Electrons with longitudinal momenta larger than 1.7 a.u. pointing towards the ion detector can overcome the extraction field and, thus, were not recorded.

Figure 1 displays the measured longitudinal momentum distribution of He^{2+} ions. A clear double-hump structure
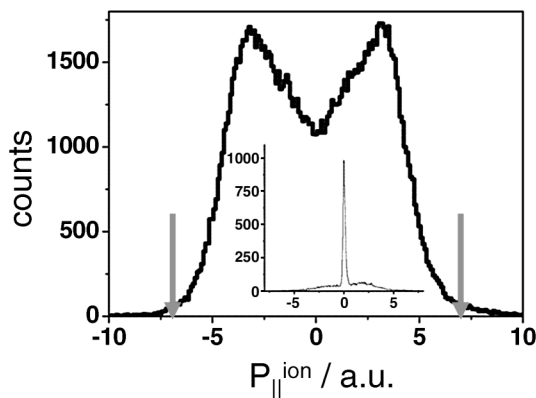
characteristic for the recollision process can be observed in the spectrum. Compared to earlier measurements on He [8,9,22] this feature appears to be much more pronounced. This difference is due to the higher intensity used in the present experiment and can be understood within the semi-classical recollision model. In [8,24] it was shown that ions emerging with small longitudinal momenta and, thus, "filling the valley" in between the two maxima, mainly originate from the recollision-induced excitation with subsequent field ionization, whereas those obtaining large momenta are created most likely by a direct (*e, 2e*)-like re-scattering event, where the relative contribution of the latter process increases with increasing intensity. The distribution extends up to the upper limits for the kinematically favorable ion momenta of $\pm 4\sqrt{U_p}$ (indicated by the arrows in Fig. 1; see [25] for details) as expected within the recollison scenario (where $U_p \propto \frac{I}{4\omega^2}$ is the so-called ponderomotive potential, I the light intensity, and ω its frequency).

Figure 2 illustrates the correlated dynamics of both emitted electrons along the laser polarization direction. Here, we have used the directly measured momentum of one electron and have recalculated the momentum of the second one from $P_\parallel^{e2} = P_\parallel^{\text{ion}} - P_\parallel^{e1}$ exploiting momentum conservation and the fact that the momentum transfer from the absorbed photons is negligible. Even though all three particles (the He^{2+} ion and two electrons) have been detected, this method was used in order to (i) increase the statistical significance of the data (the detection efficiency of about 60% for the second electron does not enter) and (ii) avoid possible ambiguities due to the dead time of the detector when both electrons arrive within less than 10 ns. As can be seen from the inset in Fig. 1, where the momentum sum of all three detected particles is shown, the

FIG. 1.   Longitudinal momentum distribution of He^{2+} ions. Arrows indicate the upper limits for the kinematically favorable ion momenta of $\pm 4\sqrt{U_p}$ [25]. Inset: Sum momentum of He^{2+} ion and two electrons detected in coincidence. Broad background below the narrow line is due to false coincidences.
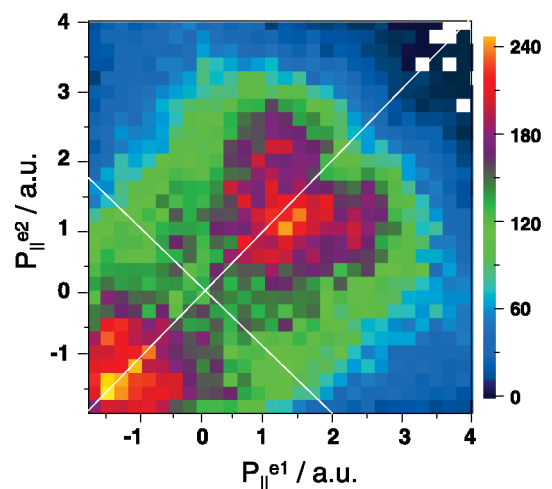
FIG. 2 (color).   Longitudinal momentum of electron one ($P_\parallel^{e1}$) versus that of electron two ($P_\parallel^{e2}$). Electrons with momenta $P_\parallel < -1.7$ a.u. are not detected (see text).

contribution of false coincidences is rather small and does not seriously disturb the spectra.

Similar to earlier results for Ne [17,18] and Ar [19,20,24] the two-electron momentum distribution shown in Fig. 2 exhibits overall maxima in the 1st and 3rd quadrants, meaning that both electrons are emitted into the same hemisphere with similar longitudinal momenta. Since the final-state electron momenta are to a large extent defined by the drift momentum acquired from the laser field, this also indicates that the electrons are emitted nearly at the same time. However, in striking contrast to all previous measurements, a clear splitting of the distribution manifests itself for helium at large $P_\parallel$ where distinct off-diagonal structures can be observed. This feature indicates that the electrons are no longer emitted with the same momentum. Though never observed in any experiment, such a behavior has been predicted by several theoretical models based on the strong-field approximation [7,26,27] as well as on the numerical solution of the TDSE for 800 nm [13,15] and 390 nm [16] laser radiation. Especially clearly it was found in an early one-dimensional numerical calculation [13], where a characteristic butter-flylike structure has been observed. However, physical reality of this feature was questioned: the intuitive explanation suggests that it originates from the Coulomb repulsion between the electrons in the final state [20], and since in a one-dimensional model the electrons cannot make way for each other by moving into the second or third spatial dimensions, the electron-electron repulsion is strongly overestimated, prohibiting emission with the same $P_\parallel$ (events on the main diagonal in Fig. 2).

The latter situation can to some extent be simulated if the transverse momenta (in the plane perpendicular to the polarization direction) of the electrons are small. Exploiting the availability of fully differential data, we plot in Fig. 3 the distribution of Fig. 2 with additional conditions on the transverse momentum $P_\perp^e$ for each of the electrons. In Fig. 3(a) only events with $P_\perp^{e1,2} \le 0.2$ a.u. are shown, whereas in Fig. 3(b) only those with $P_\perp^{e1,2} \ge$ 1.2 a.u. are presented. Even though the uncertainty due to the ion transverse momentum resolution to some extent smears out these conditions for the recalculated momentum of the second electron, clear overall differences between both panels can be observed. Whereas in Fig. 3(b) the maximum of the distribution lies on the diagonal and no noticeable splitting can be traced, Fig. 3(a) exhibits distinct off-diagonal features, which can be even distinguished in the 3rd quadrant where the events with $|P_\parallel| >$ 1.7. a.u. are missing. Thus, in good agreement with the intuitive expectations, the effect of Coulomb repulsion is strongly enhanced if electrons with negligible transverse momenta are selected.

A similar dependence of the two-electron longitudinal momentum distributions on the transverse momentum has been observed in [19,20] for Ar, where the
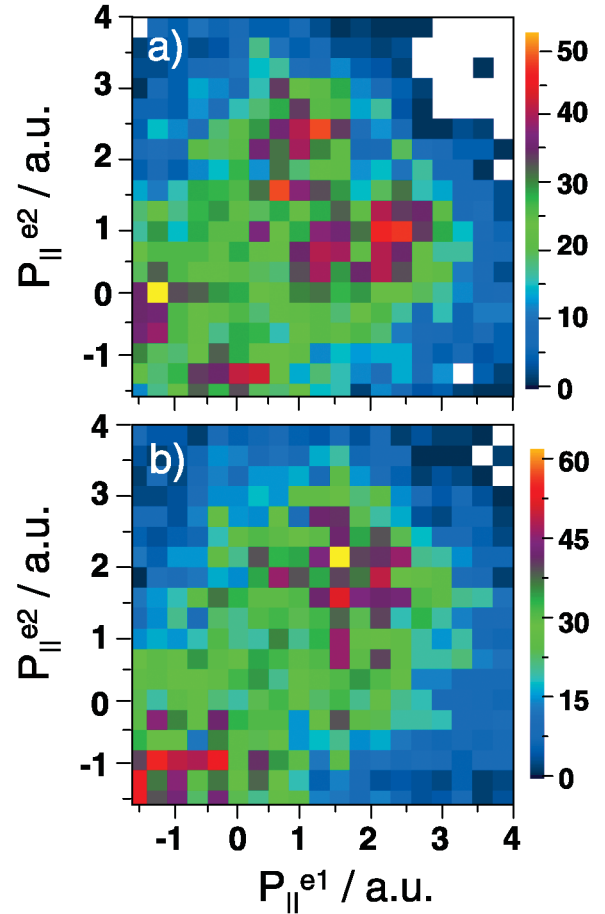
FIG. 3 (color). Same as Fig. 1 but for the transverse momentum of each electron restricted to $P_\perp^{e1,e2} \le 0.2$ a.u. (a) and $P_\perp^{e1,e2} \ge 1.2$ a.u. (b).

transverse component of only one electron was restricted. Surprisingly, however, the spectra integrated over all transverse momenta did not exhibit any noticeable splitting. Overall, the absence of clear Coulomb effects on the correlated longitudinal momentum spectra [28] caused a controversial situation for the current theoretical description of NSDI: within the *S*-matrix-based models a reasonable agreement with the existing experimental data could be achieved only if the rather unphysical contact-type electron-electron interaction has been used, while the implementation of the much more realistic Coulomb interaction resulted in the appearance of the "butterfly" structure and clear deviations from all previous experimental results [7,26,27].

The situation was extensively analyzed in [29], where the authors not only tested the role of specific types of electron-electron interactions, but also pointed out the importance of the shape of the ionic potential and differences between *p* and *s* initial electronic states. It was concluded that (i) the off-diagonal contributions due to the electron-electron repulsion are suppressed if the Coulomb potential of the ion is replaced by the contact

potential and (ii) for the latter case the round shape of the two-electron momentum distribution maximum is obtained for a *p* electron, whereas for an *s* electron a V-like shape is expected (see Fig. 11 of [29]). These predictions are in a good qualitative agreement with the findings of the present work: for He the rescattered electron (i) sees an ion potential which is closer to a pure Coulombic one than for Ne or Ar and (ii) the second emitted electron emerges from an *s* state. Correspondingly, in contrast to earlier Ne and Ar data, we observe a pronounced V shape of the two-electron momentum spectrum (see Fig. 2). Furthermore, in accordance with the explicit statement made in [26,27], the simultaneous restriction of the transverse momenta of *both* electrons to a very small value allowed us to observe a distribution very similar to the theoretical predictions for the Coulomb-type interaction.

An additional insight in the dynamics illustrated by Figs. 2 and 3 can be obtained considering the typical kinematics of a (*e*, 2*e*) recollision reaction. The *S*-matrix methods discussed above essentially describe this process within the lowest-order Born approximation [7,26,27] favoring unequal electron energy sharing after the collision. This difference, though smeared by the large drift momentum equal for both electrons, would push the correlated two-electron distribution off the $P_{\parallel}^{e1} = P_{\parallel}^{e2}$ diagonal. Restricting transverse momentum of both electrons to zero [Fig. 3(a)] enhances this effect since then the momentum transfer in the collision occurs along the laser field. Enforcing large transverse momenta for both electrons ensures that the final-state longitudinal component is mostly due to the drift momentum induced by the field which is similar for both electrons [Fig. 3(b)].

In summary, we have presented the results of a kinematically complete experiment on the prototype two-electron strong-field reaction, NSDI of He, at high intensity where the direct (*e*, 2*e*)-like ionization by the rescattering electron becomes the dominant reaction pathway. For the first time we observe a pronounced V-like shape of the correlated two-electron longitudinal momentum distribution, which can be interpreted as a consequence of Coulomb repulsion and typical (*e*, 2*e*) kinematics [30]. The essential difference between the present findings for He and earlier data on Ar and Ne can be understood in lines of recent *S*-matrix calculations [29]. Our results are in good qualitative agreement with the recent "one-plus-one"-dimensional quantum calculation (compare Fig. 2 with Fig. 6(d) of [15]), and provide benchmark data for a long-sought theoretical goal, the full three-dimensional numerical solution of the TDSE at 800 nm, which will likely become feasible in the very near future.

[1] A. Becker, R. Dörner, and R. Moshammer, J. Phys. B **38**, S753 (2005).
[2] M. Yu. Kuchiev, Sov. Phys. JETP Lett. **45**, 404 (1987).
[3] P. B. Corkum, Phys. Rev. Lett. **71**, 1994 (1993).
[4] A. Becker and F. H. M. Faisal, J. Phys. B **38**, R1 (2005).
[5] A. Becker and F. H. M. Faisal, J. Phys. B **32**, L335 (1999).
[6] R. Kopold, W. Becker, H. Rottke, and W. Sandner, Phys. Rev. Lett. **85**, 3781 (2000).
[7] S. P. Goreslavski and S. V. Popruzhenko, Opt. Express **8**, 395 (2001).
[8] V. L. B. de Jesus *et al.*, J. Phys. B **37**, L161 (2004).
[9] V. L. B. de Jesus *et al.*, J. Electron Spectrosc. Relat. Phenom. **141**, 127 (2004).
[10] S. L. Haan, L. Breen, A. Karim, and J. H. Eberly, Phys. Rev. Lett. **97**, 103008 (2006).
[11] J. S. Parker, B. J. S. Doherty, K. J. Meharg, and K. T. Taylor, J. Phys. B **36**, L393 (2003).
[12] R. Wiehle, B. Witzel, H. P. Helm, and E. Cormier, Phys. Rev. A **67**, 063405 (2003).
[13] M. Lein, E. K. U. Gross, and V. Engel, Phys. Rev. Lett. **85**, 4707 (2000).
[14] C. Ruiz, L. Plaja, L. Roso, and A. Becker, Phys. Rev. Lett. **96**, 053001 (2006).
[15] S. Prauzner-Bechcicki, K. Sacha, B. Eckhardt, and J. Zakrzewski, Phys. Rev. Lett. **98**, 203002 (2007).
[16] J. S. Parker *et al.*, Phys. Rev. Lett. **96**, 133001 (2006).
[17] R. Moshammer *et al.*, J. Phys. B **36**, L113 (2003).
[18] M. Weckenbrock *et al.*, Phys. Rev. Lett. **92**, 213002 (2004).
[19] R. Moshammer *et al.*, Phys. Rev. A **65**, 035401 (2002).
[20] M. Weckenbrock *et al.*, J. Phys. B **34**, L449 (2001).
[21] D. N. Fittinghoff, P. R. Bolton, B. Chang, and K. C. Kulander, Phys. Rev. Lett. **69**, 2642 (1992); B. Walker *et al.*, Phys. Rev. Lett. **73**, 1227 (1994).
[22] Th. Weber *et al.*, Phys. Rev. Lett. **84**, 443 (2000).
[23] R. Lafon *et al.*, Phys. Rev. Lett. **86**, 2762 (2001).
[24] B. Feuerstein *et al.*, Phys. Rev. Lett. **87**, 043003 (2001).
[25] B. Feuerstein, R. Moshammer, and J. Ullrich, J. Phys. B **33**, L823 (2000).
[26] C. Figueira de Morisson Faria, H. Schomerus, X. Liu, and W. Becker, Phys. Rev. A **69**, 043405 (2004).
[27] C. Figueira de Morisson Faria, X. Liu, and W. Becker, Phys. Rev. A **69**, 021402(R) (2004).
[28] Weak signatures of the Coulomb repulsion had been found for the transverse direction; see Ref. [18] for Ne and M. Weckenbrock *et al.*, Phys. Rev. Lett. **91**, 123004 (2003) for Ar.
[29] C. Figueira de Morisson Faria and M. Lewenstein, J. Phys. B **38**, 3251 (2005).
[30] For a complementary view of the origin of this structure, see A. Staudte *et al.*, preceding Letter, Phys. Rev. Lett. **99**, 263002 (2007).